

Temperature-Dependent Photoluminescence Properties of $\text{Ti}[\text{Ag}(\text{CN})_2]$: Formation of Luminescent Metal–Metal-Bonded Inorganic Exciplexes in the Solid State

Mohammad A. Omary and Howard H. Patterson*

Department of Chemistry, University of Maine, Orono, Maine 04469

Received July 2, 1997

The photoluminescence behavior of single crystals of $\text{Ti}[\text{Ag}(\text{CN})_2]$ has been studied as a function of temperature. The 10 K spectra show a broad emission centered at about 420 nm and two excitation maxima at 301 and 314 nm. Exciting with each of these maxima gives a different temperature dependence for the corresponding emission spectra. This result correlates with the crystal structure of the compound which indicates the presence of two environments with Ag–Ag interactions. The fact that the emission band is largely red-shifted, broad, and structureless is consistent with exciplex emission. The results of extended Hückel and ab initio calculations indicate exciplex formation in the title compound. Our theoretical calculations show a deep potential well in the excited state with a Ag–Ag equilibrium distance of 2.45 Å and a binding energy of 40.8 kcal/mol. The experimental and theoretical results in this study demonstrate the importance of excited-state Ag–Ag interactions leading to the formation of luminescent exciplexes in $\text{Ti}[\text{Ag}(\text{CN})_2]$. To our knowledge, this is the first example of exciplex formation between metal ions in the solid state for coordination compounds.

Introduction

The photophysical properties of coordination compounds of the d^{10} monovalent ions of the coinage metals continue to receive much attention. The rich luminescence properties of gold(I)^{1–8} and copper(I)^{9–15} coordination compounds have intrigued inorganic chemists in recent years. In contrast, coordination compounds of Ag(I) have received very little attention. Only a few studies^{15–17} have reported the luminescence of Ag(I) molecular coordination compounds, the first of which did not appear until 1989 by Vogler and Kunkely.¹⁶ Most

luminescence studies of Ag(I) complexes have been limited to tetranuclear clusters analogous to the $\text{Cu}_4\text{X}_4\text{L}_4$ (X, halogen; L, amine or phosphine) clusters which have been studied extensively. To our knowledge, no simple mononuclear Ag(I) complex has been reported to show luminescence prior to the title compound. The luminescent complex said to form between Ag(I) and the protein metallothionein¹⁸ has not been structurally characterized or isolated (aqueous solutions were simply prepared of the apoprotein with the addition of Ag^+ as well as Cu^+ , Au^+ , and Pt^{2+}). Luminescence of other Ag(I) species has

- (1) Weissbart, B.; Toronto, D. V.; Balch, A. L.; Tinti, D. S. *Inorg. Chem.* **1996**, *35*, 2490. Larson, L. J.; McCauley, E. M.; Weissbart, B.; Tinti, D. S. *J. Phys. Chem.* **1995**, *99*, 7218. Toronto, D. V.; Balch, A. L.; Tinti, D. S. *Inorg. Chem.* **1994**, *33*, 2507. Balch, A. L.; Catalano, V. J.; Olmstead, M. M. *Inorg. Chem.* **1990**, *29*, 585. Balch, A. L.; Fung, E. Y.; Olmstead, M. M. *Inorg. Chem.* **1990**, *29*, 3203.
- (2) Fischer, P.; Ludi, A.; Patterson, H. H.; Hewat, A. W. *Inorg. Chem.* **1994**, *33*, 62. Nagle, J. K.; LaCasce, J. H., Jr.; Dolan, P. J., Jr.; Corson, M. R.; Assefa, Z.; Patterson, H. H. *Mol. Cryst. Liq. Cryst.* **1990**, *181*, 359. Patterson, H. H.; Roper, G.; Biscoe, J.; Ludi, A.; Blom, N. J. *Lumin.* **1984**, *31/32*, 555. Markert, J. T.; Blom, N.; Roper, G.; Perregaux, A. D.; Nagasundaram, N.; Corson, M. R.; Ludi, A.; Nagle, J. K.; Patterson, H. H. *Chem. Phys. Lett.* **1985**, *118*, 258.
- (3) Striplin, D. R.; Crosby, G. A. *J. Phys. Chem.* **1995**, *99*, 11041. Striplin, D. R.; Brozik, J. A.; Crosby, G. A. *Chem. Phys. Lett.* **1994**, *231*, 159.
- (4) Koutek, M. E.; Mason, W. R. *Inorg. Chem.* **1980**, *19*, 648. Mason, W. R. *J. Am. Chem. Soc.* **1976**, *98*, 5182. Savas, M. M.; Mason, W. R. *Inorg. Chem.* **1987**, *26*, 301. Jaw, H. R.; Savas, M. M.; Rogers, R. D.; Mason, W. R. *Inorg. Chem.* **1989**, *28*, 1028. Chastain, S. K.; Mason, W. R. *Inorg. Chem.* **1982**, *21*, 3717.
- (5) McClesky, T. M.; Gray, H. B. *Inorg. Chem.* **1992**, *31*, 1733. McClesky, T. M.; Mizoguchi, T. J.; Richards, J. H.; Gray, H. B. *Inorg. Chem.* **1996**, *35*, 3434.
- (6) (a) Assefa, Z.; McBurnett, B. G.; Staples, R. J.; Fackler, J. P., Jr.; Assmann, B.; Angermaier, K.; Schmidbaur, H. *Inorg. Chem.* **1995**, *34*, 75. (b) Assefa, Z.; McBurnett, B. G.; Staples, R. J.; Fackler, J. P., Jr. *Inorg. Chem.* **1995**, *34*, 4965. (c) Assefa, Z.; Staples, R. J.; Fackler, J. P., Jr. *Inorg. Chem.* **1994**, *33*, 2790. (d) King, C.; Wang, J. C.; Khan, M. N. I.; Fackler, J. P., Jr.; *Inorg. Chem.* **1989**, *28*, 2145. (e) Khan, M. N. I.; King, C.; Heinrich, D. D.; Fackler, J. P., Jr.; Porter, L. C. *Inorg. Chem.* **1989**, *28*, 2150. (f) King, C.; Khan, M. N. I.; Staples, R. J.; Fackler, J. P., Jr. *Inorg. Chem.* **1992**, *31*, 3236. (g) Forward, J. M.; Assefa, Z.; Fackler, J. P., Jr. *J. Am. Chem. Soc.* **1995**, *117*, 9103.
- (7) Jones, W. B.; Yuan, J.; Narayanaswamy, R.; Young, M. A.; Elder, R. C.; Bruce, A. E.; Bruce, M. R. M. *Inorg. Chem.* **1995**, *34*, 1996.
- (8) Li, D.; Hong, X.; Che, C. M.; Lo, W. C.; Peng, S. M. *J. Chem. Soc., Dalton Trans.* **1993**, 2929. Li, D.; Che, C. M.; Peng, S. M.; Liu, S. T.; Zhou, Z. Y.; Mak, T. C. W. *J. Chem. Soc., Dalton Trans.* **1993**, 189. Shieh, S. J.; Li, D.; Peng, S. M.; Che, C. M. *J. Chem. Soc., Dalton Trans.* **1993**, 195. Lee, C. F.; Chin, K. F.; Peng, S. M.; Che, C. M. *J. Chem. Soc., Dalton Trans.* **1993**, 467. Che, C. M.; Kwong, H. L.; Yam, V. W. W.; Cho, K. C. *J. Chem. Soc., Chem. Commun.* **1989**, 885.
- (9) (a) Kyle, K. R.; Ryu, C. K.; DiBenedetto, J. A.; Ford, P. C. *J. Am. Chem. Soc.* **1991**, *113*, 2954. (b) Kyle, K. R.; DiBenedetto, J. A.; Ford, P. C. *J. Chem. Soc., Chem. Commun.* **1989**, 714. (c) Kyle, K. R.; Ford, P. C. *J. Am. Chem. Soc.* **1989**, *111*, 5005. (d) Kyle, K. R.; Palke, W. E.; Ford, P. C. *Coord. Chem. Rev.* **1990**, *97*, 35. (e) Døssing, A.; Ryu, C. K.; Kudo, S.; Ford, P. C. *J. Am. Chem. Soc.* **1993**, *115*, 5132. (f) Ford, P. C. *Coord. Chem. Rev.* **1994**, *132*, 129. (g) Tran, D.; Ryu, C. K.; Ford, P. C. *Inorg. Chem.* **1994**, *33*, 56. (h) Simon, J. A.; Palke, W. E.; Ford, P. C. *Inorg. Chem.* **1996**, *35*, 6413.
- (10) Hardt, D. D.; Stoll, H. J. *Z. Anorg. Allg. Chem.* **1981**, *480*, 193. Hardt, D. D.; Pierre, A. *Inorg. Chim. Acta* **1977**, *25*, L59.
- (11) Eitel, E.; Oelkrug, D.; Hiller, W.; Strähle, J. *Z. Naturforsch.* **1980**, *35b*, 1247.
- (12) Vogler, A.; Kunkely, H. *J. Am. Chem. Soc.* **1986**, *108*, 7211.
- (13) Everly, R. M.; McMillen, D. R. *J. Phys. Chem.* **1991**, *95*, 9071. Everly, R. M.; Ziessel, R.; Suffert, J.; McMillen, D. R. *J. Phys. Chem.* **1991**, *95*, 9071.
- (14) Henary, M.; Zink, J. I. *J. Am. Chem. Soc.* **1989**, *111*, 7407.
- (15) Sabin, F.; Ryu, C. K.; Ford, P. C.; Vogler, A. *Inorg. Chem.* **1992**, *31*, 1941.
- (16) Vogler, A.; Kunkely, H. *Chem. Phys. Lett.* **1989**, *158*, 74.
- (17) Henary, M.; Zink, J. I. *Inorg. Chem.* **1991**, *30*, 3111.
- (18) Stillman, M. J.; Zelazowski, A. J.; Szymanska, J.; Gasyana, Z. *Inorg. Chim. Acta* **1989**, *161*, 275.
- (19) Pedrini, C.; Jacquier, B. *Phys. Lett. A.* **1979**, *69*, 457. Pedrini, C.; Chermette, H.; Gaume-Mahn, F. *J. Lumin.* **1981**, *24/25*, 213. Pedrini, C. *Solid State Commun.* **1981**, *38*, 1237.

been limited to the free ion doped in alkali-metal halides.¹⁹ More recently, luminescence studies of different Ag(I) centers have been reported in glassy and crystalline borate²⁰ and in phosphate glasses.²¹

A recent study in our laboratory suggested that metal–metal interactions play an important role in interpreting the luminescence properties of Tl[Ag(CN)₂].²² We have reported the crystal structure of the compound which shows a layered arrangement of metal ions with Ag–Ag distances as short as 3.11 Å.²³ The experimental and theoretical results suggested the importance of *argentophilicity* in Tl[Ag(CN)₂]. Thallium–silver interactions were determined to be insignificant. Therefore, only Ag–Ag interactions are expected to affect the luminescence properties of the compound. This is in contrast to Tl[Au(CN)₂] in which both Tl–Au and Au–Au interactions are important.²⁴

In this study we report the photoluminescence spectra of Tl[Ag(CN)₂] as a function of temperature. Silver–silver interactions are analyzed to determine whether they exist between the ground or excited states of individual ions. The data in this study provide strong evidence for the formation of silver–silver-bonded exciplexes in the solid state of the compound. While exciplex formation is well-known in organic compounds,²⁵ only recently it has been recognized that such species do actually form in the excited states of transition-metal complexes. Recent examples reported involve coordination compounds of Pt(II),^{26–28} Cu(I),^{9c,29–30} Ru(II),³¹ and Ir(III).³² The exciplexes reported to form in most inorganic systems were in solution. Solid-state excimers were proposed to form in Pt(II) complexes of some aromatic ligands.²⁶ However, such excimers were proposed to

be characteristic of the π orbitals of the aromatic ligands; thus, they cannot be categorized as inorganic exciplexes. The only example of coordination compounds³³ in which exciplex formation involves metal–metal bonding has been reported by Nagle and co-workers.²⁷ The exciplex is reported to form between Pt₂(P₂O₅H₂)₄⁴⁻ and Tl(I) in solution. The title compound herein represents the first example, to our knowledge, of a metal–metal-bound exciplex in the solid state of coordination compounds.

Experimental Section

Details of the sample preparation have been discussed elsewhere.²³ Photoluminescence spectra were recorded with a PTI fluorescence spectrometer equipped with two excitation monochromators and a 75 W xenon lamp. The spectra were recorded as a function of temperature between 10 K and room temperature. Liquid helium was used as the coolant in a model Lt -3-110 Heli-Tran cryogenic liquid transfer system equipped with a temperature controller. Single crystals of high optical quality were selected using a microscope for all luminescence spectra.

Computational Details

Extended Hückel molecular orbital calculations were performed using the FORTICON8 program (QCMP011). Relativistic parameters were used for all atoms, and the details are described elsewhere.²² The atom separations used in the calculations were according to the crystal structure of Tl[Ag(CN)₂].²³ The program allows for excited-state calculations which were carried out for the title compound.

Ab initio calculations on the restricted Hartree–Fock level were performed using the STO-3G basis set available in the SPARTAN program (Version 4.1.1, Wave function Inc., Irvine, CA). To reduce the calculation time and to cope with the complexity of the model species, only single-point energy calculations (no geometry optimization) were performed. The input geometry corresponds to the structure minimized by extended Hückel calculations.²³ Bond order analysis was performed according to the Mulliken³⁴ and Löwdin³⁵ methods as taken directly from the output file. In the former method, the electron density is partitioned equally between the atoms involved in a bond. The latter method, on the other hand, uses the overlap between atomic functions to partition the charge.

Results and Discussion

1. Photoluminescence Spectra. Figure 1 shows the photoluminescence emission and excitation spectra of Tl[Ag(CN)₂] at 10 K. Two prominent maxima at 301 and 314 nm appear in the excitation spectrum. The most important feature in the excitation spectrum of Tl[Ag(CN)₂] is the low energies of the peaks. The energies of the excitation peaks of Tl[Ag(CN)₂] at 10 K are much lower than the absorption band energies of (*n*-Bu)₄N[Ag(CN)₂] observed by Mason, a case where very long silver–silver distances are expected due to the presence of the bulky cation.³⁶ A solid film of (*n*-Bu)₄N[Ag(CN)₂] at 40 K gave rise to several absorption peaks between 42.6 and 51.2 × 10³ cm⁻¹ while, for frozen EPA solutions (77 K), all absorption bands had energies of 42.9 × 10³ cm⁻¹ and higher.³⁶ No luminescence data were reported in that study. It should also be noted that in the free Ag⁺ ion, the 4d⁹5s¹ excited state is located 39164 cm⁻¹ above the 4d¹⁰ ground state^{37,38} and the

- (20) Meijerink, A.; van Heek, M. M. E.; Blasse, G. *J. Phys. Chem. Solids* **1993**, *54*, 901.
- (21) Mesnaoui, M.; Maazaz, M.; Parent, C.; Tanguy, B.; LeFlem, G. *Eur. J. Solid State Inorg. Chem.* **1992**, *29*, 1001.
- (22) Omary, M. A.; Patterson, H. H.; Shankle, G. *Mol. Cryst. Liq. Cryst.* **1996**, *284*, 399.
- (23) Omary, M. A.; Webb, T. R.; Assefa, Z.; Shankle, G. E.; Patterson, H. H. *Inorg. Chem.*, in press.
- (24) Assefa, Z.; DeStefano, F.; Garepapaghi, M. A.; LaCasce, J. H., Jr.; Ouellette, S.; Corson, M. R.; Nagle, J. K.; Patterson, H. H. *Inorg. Chem.* **1991**, *30*, 2868.
- (25) (a) Lowry, T. H.; Schuller-Richardson, K. *Mechanism and Theory in Organic Chemistry*; Harper & Row: New York, 1981; pp 919–925. (b) Turro, N. J. *Modern Molecular Photochemistry*; Benjamin/Cummings: Menlo Park, CA, 1978; pp 135–146. (c) Lamola, A. A. In *Energy Transfer and Organic Photochemistry*; Lamola, A. A., Turro, N. J., Eds.; Wiley-Interscience: New York, 1969; pp 54–60. (d) *The exciplex*; Gordon, M., Ware, W. R., Eds; Academic Press: New York, 1975. (e) Kopecky, J. *Organic Photochemistry: A Visual Approach*; VCH: New York, 1991; pp 38–40. (f) Michl, J.; Bonacic-Koutecky, V. *Electronic Aspects of Organic Photochemistry*; Wiley: New York, 1990; pp 274–286.
- (26) Bailey, J. A.; Hill, M. G.; Marsh, R. E.; Miskowski, V. M.; Schaefer, W. P.; Gray, H. B. *Inorg. Chem.* **1995**, *34*, 4591. Miskowski, V. M.; Houlding, V. H. *Inorg. Chem.* **1989**, *28*, 1529.
- (27) (a) Clodfelter, S. A.; Doede, T. M.; Brennan, B. A.; Nagle, J. K.; Bender, D. P.; Turner, W. A.; LaPunzia, P. M. *J. Am. Chem. Soc.* **1994**, *116*, 11379. (b) Nagle, J. K.; Brennan, B. A. *J. Am. Chem. Soc.* **1988**, *110*, 5931.
- (28) (a) Chan, C.-W.; Lai, T.-F.; Che, C.-M.; Peng, S.-M. *J. Am. Chem. Soc.* **1993**, *115*, 11379. (b) Kunkely, H.; Vogler, A. *J. Am. Chem. Soc.* **1990**, *112*, 5625.
- (29) Stevenson, K. L.; Knorr, D. W.; Horváth, A. *Inorg. Chem.* **1996**, *35*, 835. Horváth, A.; Wood, C. E.; Stevenson, K. L. *Inorg. Chem.* **1994**, *33*, 5351. Horváth, A.; Wood, C. E.; Stevenson, K. L. *J. Phys. Chem.* **1994**, *98*, 6490. Horváth, A.; Stevenson, K. L. *Inorg. Chem.* **1993**, *32*, 2225.
- (30) Stacy, E. M.; McMillin, D. R. *Inorg. Chem.* **1990**, *29*, 393. Palmer, C. E. A.; McMillin, D. R.; Kirmaier, C.; Holten, D. *Inorg. Chem.* **1987**, *26*, 3167.
- (31) Ayala, N. P.; Demas, J. N.; DeGraff, B. A. *J. Phys. Chem.* **1989**, *93*, 4104. Ayala, N. P.; Demas, J. N.; DeGraff, B. A. *J. Am. Chem. Soc.* **1988**, *110*, 1523.
- (32) Ayala, N. P.; Demas, J. N.; DeGraff, B. A. *J. Am. Chem. Soc.* **1988**, *110*, 1523.

- (33) [CuCu]²⁺ excimers and [CuAg]²⁺ exciplexes have been reported to form in β'' -alumina doped with copper ions (Hollingsworth, G.; Barrie, J. D.; Dunn, B.; Zink, J. I. *J. Am. Chem. Soc.* **1988**, *110*, 6569) and with copper and silver ions (Barrie, J. D.; Dunn, B.; Zink, J. I. *J. Am. Chem. Soc.* **1990**, *112*, 5701). The doped species, however, were simple Cu⁺ and Ag⁺ ions and not coordinated compounds.
- (34) Mulliken, R. S. *J. Chem. Phys.* **1955**, *23*, 1833, 1841, 2338, and 2345.
- (35) Löwdin, P. O. *Svensk Kem. Tidskr.* **1955**, *67*, 383. Löwdin, P. O. *J. Chem. Phys.* **1953**, *21*, 374. Foster, J. P.; Weinhold, F. *J. Am. Chem. Soc.* **1980**, *102*, 7211. Reed, A. E.; Weinstock, R. B.; Weinhold, F. *J. Chem. Phys.* **1985**, *83*, 735.
- (36) Mason, W. R. *J. Am. Chem. Soc.* **1973**, *95*, 3573.
- (37) Moore, C. E. *Atomic Energy Levels*; Nat. Bur. Stand.: Washington, DC, 1958; Circ. 467, Vol. III. Orgel, L. E. *J. Chem. Soc.* **1958**, 4186.

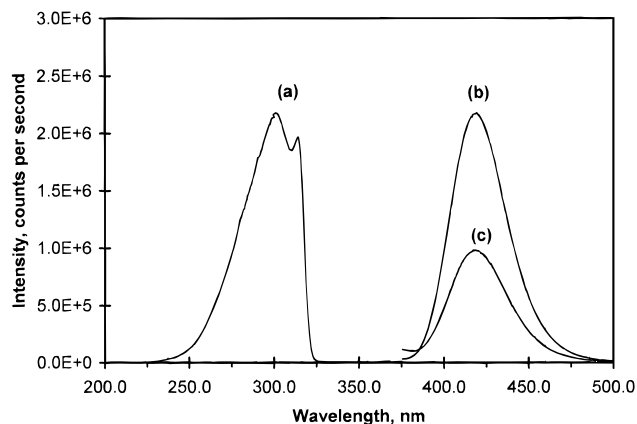


Figure 1. Luminescence spectra of $\text{Tl}[\text{Ag}(\text{CN})_2]$ at 10 K. (a) is the excitation spectrum monitoring the emission at 418 nm; (b) and (c) are the emission spectra with excitation at 301 and 318 nm, respectively.

corresponding absorption band was observed at $44.7 \times 10^3 \text{ cm}^{-1}$ in aqueous solutions of Ag^+ .³⁸ Moreover, the $4d-5s$ bands of Ag^+ doped in alkali-metal halide matrices occurred in the same energy range.³⁹ In $\text{Tl}[\text{Ag}(\text{CN})_2]$, the 31.8 and $33.2 \times 10^3 \text{ cm}^{-1}$ energies of the two excitation maxima are significantly lower than the values of these other systems.

Emission spectra of $\text{Tl}[\text{Ag}(\text{CN})_2]$ were scanned using both 301 and 318 nm excitation wavelengths. The 318 nm excitation was chosen because it has less contribution from the 301 nm signal than 314 nm. Figure 1 shows that the emission bands occur at 419 and 418 nm with excitation at 301 and 318 nm, respectively. We assigned this emission to a spin-forbidden transition from a triplet excited-state on the basis of our lifetime data.²² These wavelength values represent a large red shift from the lowest energy emission band observed for Ag^+ doped in NaCl (which was also spin-forbidden) assigned to the $^3E_g(5s) \rightarrow ^1A_{1g}(4d)$ transition observed at 250 nm.¹⁹ The energies of both emission and excitation luminescence bands of $\text{Tl}[\text{Ag}(\text{CN})_2]$ are too low to be assigned to isolated $\text{Ag}(\text{CN})_2^-$ centers. Therefore, Ag–Ag interactions must be responsible for the low energy values of the luminescence bands.

Figure 2 shows the temperature-dependent emission spectra of a single $\text{Tl}[\text{Ag}(\text{CN})_2]$ crystal using 318 nm excitation. Figure 2 shows that the $\text{Tl}[\text{Ag}(\text{CN})_2]$ emission undergoes a red-shift with the stepwise decrease of temperature. The emission peak located at 418 nm at 10 K gradually shifts to shorter wavelengths and reaches 403 nm at 195 K. This represents an average shift of about $5 \text{ cm}^{-1}/\text{K}$. A similar energy shift was obtained for the emission spectra scanned with 301 nm excitation. A shift of the luminescence bands to lower energies upon cooling is a well-known spectroscopic characteristic for compounds with a layered structure. Yersin and Gliemann established that lowering the temperature results in thermal contraction of the in-chain or in-plane M–M distances in low-dimensional layered compounds.⁴⁰ Other studies in the literature support this argument. For example, a recent neutron powder diffraction study of $\text{Tl}[\text{Au}(\text{CN})_2]$ has indicated a decrease of Au–Au distances with decreasing temperature.^{2a} Also, Gray and co-

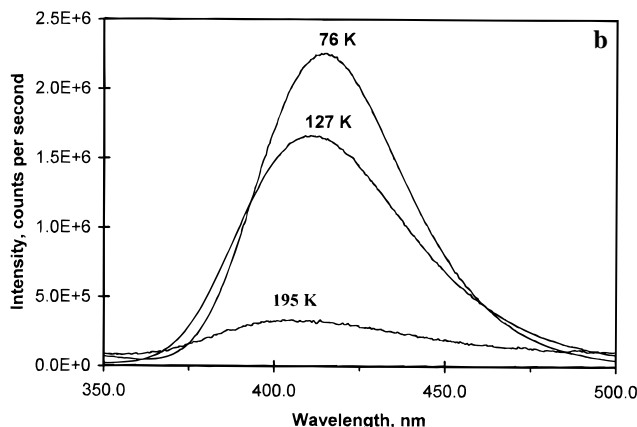
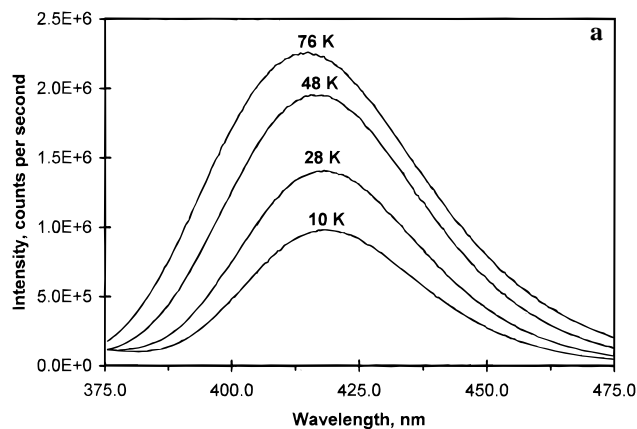


Figure 2. Emission spectra of $\text{Tl}[\text{Ag}(\text{CN})_2]$ as a function of temperature (a) in the 10–76 K temperature range and (b) in the 76–127 K temperature range. The spectrum at 195 K in (b) is magnified $10\times$. workers have noted the contraction of the stacks of the linear-chain molecule $\text{Pt}(\text{bpy})\text{Cl}_2$ ($\text{bpy} = 2,2'$ -bipyridine) upon progressive cooling. The shorter Pt–Pt distances at lower temperatures have resulted in a red shift of the luminescence band of the compound.⁴¹

We attribute the observed luminescence of $\text{Tl}[\text{Ag}(\text{CN})_2]$ to the presence of two sites in the crystal structure with both sites having relatively short nearest-neighbor Ag–Ag distances. The shortest Ag–Ag contact of 3.11 \AA in the environment of one site, Ag(1), is well below the summed van der Waals radii of two silver atoms ($r_{\text{VDW}} = 1.70 \text{ \AA}$ for silver).⁴² The nearest-neighbor Ag–Ag separation in the environment of the other site, Ag(2), is 3.53 \AA which is only slightly above the van der Waals limit of 3.40 \AA . It is interesting to note that Holt and co-workers found that, in tetrameric halo-amine clusters of Cu(I), low-energy luminescence was observed only from clusters with Cu–Cu distances below the summed van der Waals radii of two copper ions.⁴³ Ab initio studies of similar compounds by Ford et al. supported this argument qualitatively.⁴⁴ The study herein, therefore, suggests that the same argument is likely true for Ag(I) coordination compounds. The luminescence bands depicted in Figure 1 are assigned to Ag–Ag interactions in the environments of both Ag(1) and Ag(2) sites in the crystal structure of $\text{Tl}[\text{Ag}(\text{CN})_2]$.

(38) Jørgensen, C. K. *Absorption Spectra and Chemical Bonding in Complexes*; Pergamon Press: Oxford, U.K., 1962. Volbert, F. Z. *Physik. Chem.* **1930**, A149, 382.

(39) Fussgaenger, K.; Martiensen, W.; Bilz, H. *Phys. Stat. Solidi* **1965**, 12, 383. Dreybrodt, W.; Fussgaenger, K. *Phys. Stat. Solidi* **1966**, 18, 133.

(40) Yersin, H.; Gliemann, G. *Ann. N.Y. Acad. Sci.* **1978**, 313, 539. Gliemann, G.; Yersin, H. *Struct. Bonding* **1985**, 62, 87 and references therein.

(41) Connick, W. B.; Henling, L. M.; Marsh, R. E.; Gray, H. B. *Inorg. Chem.* **1996**, 35, 6261.

(42) Bondi, A. *J. Chem. Phys.* **1964**, 41, 3199.

(43) Rath, N. P.; Holt, E. M.; Tanimura, K. *Inorg. Chem.* **1985**, 24, 3934; *J. Chem. Soc., Dalton Trans.* **1986**, 2303. Rath, N. P.; Maxwell, J. L.; Holt, E. M. *J. Chem. Soc., Dalton Trans.* **1986**, 2449. Tompkins, J. A.; Maxwell, J. L.; Holt, E. M. *Inorg. Chim. Acta* **1987**, 127, 1.

(44) Vitale, M.; Ryu, C. K.; Palke, W. E.; Ford, P. C. *Inorg. Chem.* **1994**, 33, 561.

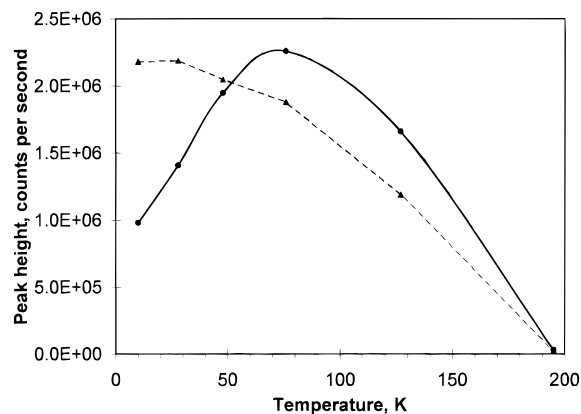


Figure 3. Temperature-dependence of the intensities of $\text{Ti}[\text{Ag}(\text{CN})_2]$ emission bands scanned with excitation wavelengths of 318 nm (solid line) and 301 nm (dashed line). The lines are guides for the eye.

The intensity of the $\text{Ti}[\text{Ag}(\text{CN})_2]$ emission bands show an interesting temperature behavior for the spectra scanned with 318 nm excitation. While the band intensity increases as the crystal is progressively heated between 10 and 76 K (Figure 2a), a large decrease of the intensity is observed upon heating to higher temperatures (Figure 2b). The spectrum recorded at 195 K is actually magnified 10× in Figure 2b. No luminescence is observed at all at room temperature. A rather different temperature behavior is obtained for emission spectra excited with 301 nm. Figure 3 shows the emission intensity versus temperature for the spectra scanned with the two excitation maxima. Emission spectra with 301 nm excitation show a general decrease in intensity upon progressive heating.

The existence of two excitation maxima, each of which has a different temperature behavior for its corresponding emission spectra, is consistent with the presence of two different sites with close Ag–Ag distances in the crystal structure of the compound. The shorter Ag–Ag distance in the Ag(1) environment leads to a greater interaction between neighboring $\text{Ag}(\text{CN})_2^-$ ions in this environment relative to the Ag(2) environment. We, consequently, assign the luminescence excitation peak at 314 nm and its corresponding emission to result from Ag–Ag interactions surrounding Ag(1) while the 301 nm peak is assigned to the Ag(2) environment.

The complicated temperature dependence of the intensities of the emission bands of the title compound is explained in view of the aforementioned assignment. First let us discuss the temperature dependence of the emission assigned for the Ag(1) environment, namely the spectra excited with 318 nm (Figure 2). The increase of emission intensity as the temperature is increased from 10 to 76 K (Figure 2a) can be explained by thermal decay processes from higher excited states. Such pathways are known to be thermally activated. Therefore, by an increase of the temperature in the 10–76 K range, the triplet state responsible for the emission becomes more populated as the energy migrates through the lattice from higher excited states (such as the singlet excited state) leading to increased triplet emission. On the other hand, as the temperature is increased above 76 K toward room temperature (Figure 2b), nonradiative processes such as multiphonon relaxation to the ground state become more dominant thus leading to depletion of the emission. The high frequencies of the cyanide stretching bands (ca. 2120 cm^{-1})²³ facilitate such decay process. A similar temperature dependence was observed for the emission bands

of $\text{K}[\text{Au}(\text{CN})_2]$, whose lowest-energy emission band reached a maximum at 160–180 K.⁴⁵

The temperature behavior of the emission spectra of the Ag(2) environment cannot be explained by decay processes from higher excited states because the emission intensity did not gradually increase above 10 K (Figure 3). Instead, it appears that nonradiative processes are the dominant pathways responsible for the decreasing intensities above 10 K in the emission spectra scanned with 301 nm. The contrasting temperature behavior between the two emitting sites of the title compound is surprising. However, an analogy can be made with tetracyanoplatinate(II) salts for which the temperature behavior of their emission bands has been well-characterized by Yersin and Gliemann.⁴⁰ For example, $\text{KLi}[\text{Pt}(\text{CN})_4] \cdot 2\text{H}_2\text{O}$ showed a temperature behavior similar to that observed in Figure 2 as the low-energy triplet emission reached a maximum around 75 K for that compound. The activation energies for the decay from higher-energy excitons to the triplet state were determined experimentally, and the results demonstrated that, in general, compounds with longer Pt–Pt distances gave rise to higher activation energy values than compounds with shorter Pt–Pt distances.⁴⁰ On the basis of this argument, a lower energy barrier should be associated with the decay process to the triplet emissive state of Ag(1) relative to Ag(2) since the nearest-neighbor Ag atoms are within a shorter distance (3.11 Å) in the former. It is also noted that the Stokes shift is smaller for the Ag(1) emission. Therefore, the energy gap for the migration of the excitation energy to the emissive state is smaller for Ag(1). Consequently, such migration proceeds with relative ease in the Ag(1) environment leading to increasing population of the triplet state and thus to increasing intensity between 10 and 76 K. The corresponding energy gap for Ag(2) is larger; thus, the migration of the excitation energy becomes more difficult to proceed and the characteristic emission intensity does not increase with increasing temperature.

Exciting with different excitation wavelengths has resulted in rather similar emission spectra. The two emission spectra in Figure 1 have a very similar band shape and almost identical maxima. Even though the two emission bands expected from the spectra obtained with different excitation wavelengths were not resolved, the different behavior toward temperature, in essence, resolves the two emissions.

2. Molecular Orbital Calculations. Since the luminescence data suggest that silver–silver interactions play a central role in the luminescence behavior of $\text{Ti}[\text{Ag}(\text{CN})_2]$, theoretical calculations have been designed to model the lattice environments in which short Ag–Ag contacts are observed in the crystal structure. Calculations for the thermodynamic stability of the ions in these environments are described elsewhere.²³ The calculations herein focus on relating Ag–Ag interactions to the optical properties of $\text{Ti}[\text{Ag}(\text{CN})_2]$. Three $\text{Ag}(\text{CN})_2^-$ ions are present in the Ag(1) environment with the ion in the center separated from the other two terminal ions by 3.11 Å.²³ A trimer model of $\text{Ag}(\text{CN})_2^-$ ions is, therefore, used to describe the Ag(1) environment. On the other hand, five $\text{Ag}(\text{CN})_2^-$ ions are present in the Ag(2) environment with two sets of Ag–Ag contacts. The shortest contact is 3.53 Å for two of the ions surrounding the central Ag(2) atom, while the other terminal ions are separated by 3.89 Å from Ag(2). The 3.89 Å separation can be ignored because it is well above the sum of the van der Waals radii for two Ag atoms. Therefore, the Ag(2) environment can also be approximated as a trimer with a Ag–Ag separation of 3.53 Å, which is in the vicinity of the van der Waals limit. Molecular orbital calculations have been performed

(45) Nagasundaram, N.; Roper, G.; Biscoe, J.; Chai, J. W.; Patterson, H. H.; Blom, N.; Ludi, A. *Inorg. Chem.* **1986**, *25*, 2947.

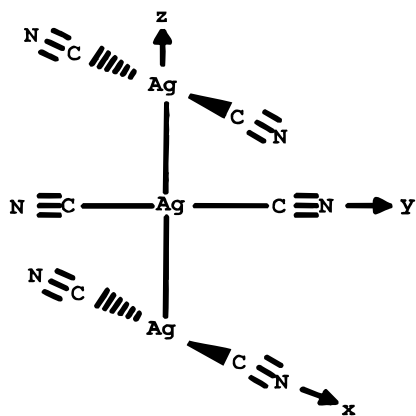


Figure 4. Setup of the axes for the trimer model for which the extended Hückel calculations were carried out. Note the cyanides of the two terminal silvers are on the *x*-axis, which is perpendicular to the plane of the page.

Table 1. Results of Relativistic Extended Hückel Calculations of the HOMO–LUMO Gap and Total Energy for Interacting $\text{Ag}(\text{CN})_2^-$ Ions in the Trimers Representing the Environments of the Ag(1) and Ag(2) Sites in the Crystal Structure of $\text{Tl}[\text{Ag}(\text{CN})_2]$

site	Ag(1)	Ag(2)
Ag–Ag dist, Å	3.11	3.53
HOMO–LUMO gap, eV	3.64	3.80
tot. energy, eV	–1491.88	–1492.22

for these two trimer models using the extended Hückel method in order to evaluate the differences between the two emitting sites. Approximations were made that all $\text{Ag}(\text{CN})_2^-$ ions were linear and perpendicular to each other in both models.⁴⁶ The trimer model used in our calculations is shown in Figure 4.

Table 1 summarizes the important results of our extended Hückel calculations for the two sites described above. The data in Table 1 indicate a smaller HOMO–LUMO gap for the trimer representing the Ag(1) environment. This confirms the above assignment of the luminescence excitation peak at 314 nm and its corresponding emission as resulting from Ag–Ag interactions surrounding Ag(1), while the 301 nm peak is assigned to the Ag(2) environment. The energy difference between the HOMO–LUMO gaps of the two trimers (0.16 eV) is in excellent agreement with the experimental energy difference between the two excitation maxima (ca. $1.38 \times 10^3 \text{ cm}^{-1} = 0.17 \text{ eV}$). Therefore, the resolution of the excitation spectrum of $\text{Tl}[\text{Ag}(\text{CN})_2]$ has allowed for differentiation between two similar emitting sites of the same compound. This has not been commonly encountered in the photophysical investigations of coordination compounds.^{47,48}

Figure 5 shows that the HOMO–LUMO gap decreases as the Ag–Ag distance decreases in the trimer model. A good fit

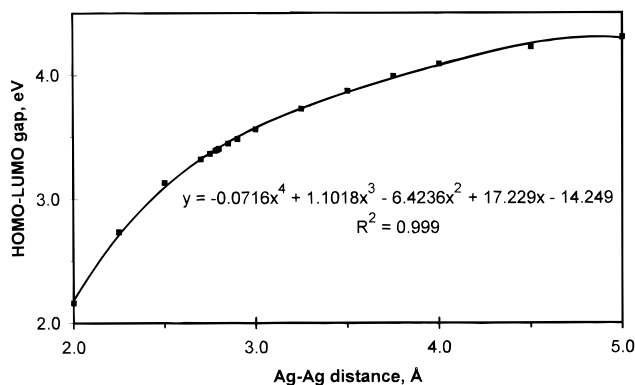


Figure 5. Change of the HOMO–LUMO gap as a function of the Ag–Ag distance in the $[\text{Ag}(\text{CN})_2^-]_3$ trimer model describing silver–silver interactions in the $\text{Tl}[\text{Ag}(\text{CN})_2]$ crystal as obtained from relativistic extended Hückel calculations.

to this decrease was obtained using a fourth order polynomial equation. A similar fit was reported by Fackler et al. in gold (I) phosphadamantane complexes.^{6a} This demonstrates the sensitivity of the optical properties of Ag(I) compounds to Ag–Ag interactions. Also, Figure 5 provides a theoretical support for the red shift observed in the luminescence band of the title compound upon progressive cooling since shorter Ag–Ag distances are expected at lower temperatures.

3. Exciplex Model. The observation of a rather broad, red-shifted, and structureless emission for $\text{Tl}[\text{Ag}(\text{CN})_2]$ is reminiscent of excimer and exciplex emissions observed in planar aromatic compounds such as pyrene.²⁵ Although most of the investigations of excimer-forming organic molecules have been in solution, the few solid-state investigations suggest that the molecules must be stacked in columns or arranged in pairs with an interplanar distance of less than 3.5 Å (the C–C distance in graphite) in order for the excimers to form.⁴⁹ The layered structure of $\text{Tl}[\text{Ag}(\text{CN})_2]$ satisfies this condition.

The very low energies of the luminescence bands of $\text{Tl}[\text{Ag}(\text{CN})_2]$ cannot be attributed to silver–silver bonding in the ground state because Ag(I) ions have filled 4d orbitals which gives a net bonding of zero if these orbitals interact in the ground state. This is especially true for silver compounds compared to gold compounds because the relativistic effects are less important in silver than gold. Relativistic effects allow significant mixing between the 5d orbitals and the 6s and 6p orbitals of gold. Some studies suggested that mixing of 5s and 5p orbitals in the ground state could provide a pathway for Ag–Ag interactions in tetranuclear silver (I) complexes.¹⁶ However, in a theoretical/experimental study Cotton et al. showed that even in dinuclear silver(I) compounds of bridged ligands in which a very short Ag–Ag distance (2.70 Å) is enforced by the geometry, little or no bonding takes place between Ag(I) centers.⁵⁰

The largely red-shifted luminescence bands in $\text{Tl}[\text{Ag}(\text{CN})_2]$ cannot result from ground-state interactions between Ag(I) ions by s–d or p–d mixing. Therefore, such interactions have to be present in the excited states. It is interesting to note that the Ag(1) and Ag(2) environments have rather different Ag–Ag ground-state distances. Nevertheless, their emission energies are virtually identical which indicates that the Ag–Ag interactions are in the excited states. A similar conclusion was reached by Henary and Zink in interpreting the lower emission energy associated with the cube isomer relative to the chair isomer of the tetrameric cluster $\text{Ag}_4\text{I}_4(\text{PPh}_3)_4$ despite the fact that very little difference in the ground-state Ag–Ag distance exists between the two isomers.¹⁷ Since two isomers with similar Ag–

- (46) The crystal structure shows a little deviation from linearity for the $\text{Ag}(\text{CN})_2^-$ ions of Ag(3), which represent the terminal ions in both models. The C–Ag–C angle in that site is $172.3(1)^\circ$. The ions in the Ag(1) and Ag(2) sites were linear as both sites lie on inversion centers. The crystal structure also shows that the dihedral angle in the Ag(1) site is 98° ; thus, a perpendicular geometry is a valid assumption too.
- (47) Lanthanide ion excitation spectra that are sensitive to the environment have been used in biological systems. See: Horrocks, W. DeW., Jr.; Sundic, D. R. *Acc. Chem. Res.* **1981**, *14*, 384. Richardson, F. S. *Chem. Rev. (Washington, D.C.)* **1982**, *82*, 541. Horrocks, W. DeW., Jr.; Albin, M. *Prog. Inorg. Chem.* **1984**, *31*, 1.
- (48) For a recent example, see: Bruno, J.; Horrocks, W. DeW., Jr.; Beckingham, K. *Biophys. Chem.* **1996**, *63*, 1–16.
- (49) Ferguson, J. *J. Chem. Phys.* **1958**, *28*, 765. Stevens, B. *Spectrochim. Acta* **1962**, *18*, 439.
- (50) Cotton, F. A.; Feng, X.; Matusz, M.; Poli, R. *J. Am. Chem. Soc.* **1988**, *110*, 7077.

Table 2. Summary of the Results of Extended Hückel Calculations for the Ground and Excited States of the $[\text{Ag}(\text{CN})_2^-]_3$ Model (Figure 4)

	species		
	$\text{Ag}(\text{CN})_2^-$ isolated ions	$[\text{Ag}(\text{CN})_2^-]_3$ (trimer)	$*[\text{Ag}(\text{CN})_2^-]_3$ (exciplex)
Ag–Ag equilibrium dist, Å	6.00	2.79	2.45
binding energy, eV	0.00	0.60	1.77
HOMO–LUMO gap, eV	4.35	3.40	3.11
OP(Ag–Ag) ^a	–0.001	0.034	0.0712
OP(Ag–C) ^a	0.258	0.237	0.216

^a OP = overlap population. Values are listed for bonds with the central silver atom.

Ag distances yielded quite different emissions in that study while in our study two different sites with quite different ground-state Ag–Ag distances yielded almost identical emission energies, it seems to us that there is a general tendency for Ag–(I) species to interact strongly in their excited states instead of their ground states. Given the excited-state nature of Ag–Ag interactions, the ground-state silver–silver distance plays little role in such interactions as well as the luminescence spectra.

The other experimental observation which provides strong evidence for an exciplex model for $\text{Ti}[\text{Ag}(\text{CN})_2]$ is the very large Stokes shifts observed for the emission bands. Large Stokes shifts are indicative of highly distorted excited states. This is clearly reflected by the broadness of the luminescence bands observed in Figure 1. Upon a one-photon excitation, the bond order should increase according to the exciplex model by 1.00 for two interacting ions (excimer) and by 0.50 for three interacting ions (two Ag–Ag contacts).

To evaluate the relative importance of ground-state versus excited-state Ag–Ag interactions, extended Hückel calculations have been carried out for the ground and the first excited state of the trimer model of the title compound (Figure 4); the results are summarized in Table 2. The results of the calculations show that a potential well forms for the ground state of the $[\text{Ag}(\text{CN})_2^-]_3$ trimer with a short Ag–Ag equilibrium distance of 2.79 Å. Moreover, a larger binding energy, smaller HOMO–LUMO gap, greater Ag–Ag overlap population, and a smaller Ag–C overlap population are obtained in the $[\text{Ag}(\text{CN})_2^-]_3$ trimer relative to isolated $\text{Ag}(\text{CN})_2^-$ ions. Ground-state Ag–Ag interactions are also supported by our ab initio calculations. Single-point calculations have been carried out for the trimer model depicted in Figure 4 at silver–silver distances of 2.79, 3.11, and 3.53 Å. The 2.79 Å distance corresponds to the equilibrium Ag–Ag distance obtained from the extended Hückel calculation. The 3.11 and 3.53 Å distances correspond to the Ag–Ag separations in the environments of Ag(1) and Ag(2) in the crystal structure of $\text{Ti}[\text{Ag}(\text{CN})_2]$. Bond order analysis was performed using ab initio calculations which indicated that both the Mulliken and Löwdin bond orders are positive and relatively large (0.4–0.5) for Ag–Ag bonds in the trimer. Details are available in the Supporting Information.

Excited-state Ag–Ag interactions can be understood from analysis of the composition of the HOMO and LUMO orbitals of the $[\text{Ag}(\text{CN})_2^-]_3$ trimer. Since silver–silver interactions seem to be the dominant factor in determining the photoluminescence behavior of $\text{Ti}[\text{Ag}(\text{CN})_2]$, vide supra, special attention should be given to the composition of the HOMO and the LUMO with respect to the silver atoms in each site. This has been carried out using both extended Hückel and ab initio calculations at the equilibrium Ag–Ag separation of 2.79 Å. Equations 1 and 2 show the composition of both the HOMO and the LUMO, respectively, according to the extended Hückel calculations. The

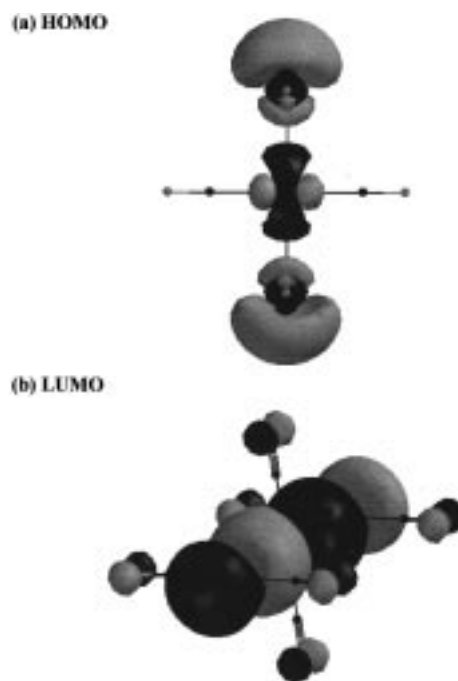


Figure 6. Surface drawing of the HOMO (a) and the LUMO (b) orbitals of the $[\text{Ag}(\text{CN})_2^-]_3$ trimer model according to ab initio calculations using the STO-3G basis set. The Ag–Ag distance is 2.79 Å, which corresponds to the minimized structure of the ground state (Table 2). Note the HOMO has an antibonding character and the LUMO has a bonding character with respect to Ag–Ag bonds (the interaction in the LUMO occurs between the p_z orbitals of Ag atoms).

“c” and “t” subscripts denote the central and terminal silver atoms, respectively.

$$\begin{aligned} \text{HOMO} = (1/0.32)\{ & 0.26 s(\text{Ag}_c) - 0.34 d_{z^2}(\text{Ag}_c) - \\ & 0.17 s(\text{Ag}_{t1}) + 0.2 d_{z^2}(\text{Ag}_{t1}) - 0.17 s(\text{Ag}_{t2}) + \\ & 0.2 d_{z^2}(\text{Ag}_{t2}) \} \quad (1) \end{aligned}$$

$$\begin{aligned} \text{LUMO} = (1/0.13)\{ & 0.15 p_z(\text{Ag}_c) - 0.23 p_z(\text{Ag}_{t1}) - \\ & 0.23 p_z(\text{Ag}_{t2}) \} \quad (2) \end{aligned}$$

The setup of the axes in the calculations was such that the central silver atom lies at the origin and the z-axis passes through all three silver atoms as shown in Figure 4. Taking this into consideration, it is obvious that the HOMO has an antibonding character while the LUMO has a bonding character with respect to the Ag–Ag bonds. This result is confirmed by our ab initio calculations for the same model. Figure 6 shows the surfaces of the HOMO and the LUMO orbitals as plotted from the output of the ab initio calculations. Similar surfaces were obtained for trimers with Ag–Ag separations as in the crystal structure. The surfaces depicted in Figure 6 qualitatively describe the bonding interactions between Ag atoms inferred from eqs 1 and 2 above. Both the ab initio and the extended Hückel calculations, therefore, produce similar qualitative results for the $[\text{Ag}(\text{CN})_2^-]_3$ model. The antibonding character of the HOMO and the bonding character of the LUMO with respect to Ag–Ag bonds are evident in Figure 6. This is an interesting situation because it means that upon excitation of an electron from the HOMO to the LUMO, a net Ag–Ag bonding results; i.e., the interaction of silver dicyanide monomer units in their excited states leads to a net increase in the bond order with respect to silver. This leads to the formation of exciplexes between the interacting silver dicyanide units.

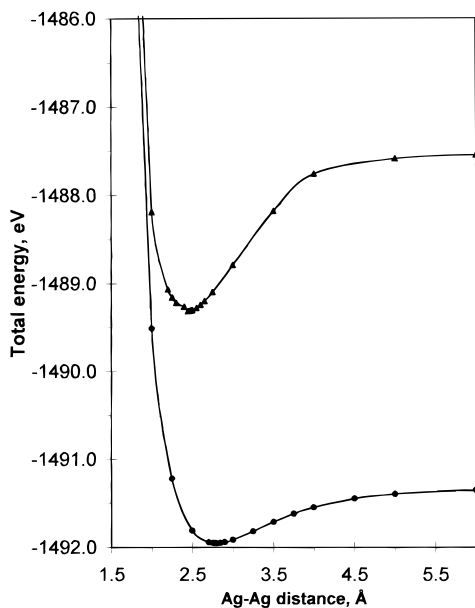


Figure 7. Potential energy curve of both the ground state and the first excited state of the $[\text{Ag}(\text{CN})_2^-]_3$ trimer model. The minimum of the potential well in the excited state represents the exciplex.

To further elucidate the exciplex model, we have performed extended Hückel calculations for the excited state of the $[\text{Ag}(\text{CN})_2^-]_3$ model trimer. Such calculations are important because they account for the adjustment of the nuclei in response to the absorption of light. Since the HOMO–LUMO transition is expected to affect the bond order, nuclear adjustment should be significant as the excited state is expected to be largely distorted from the ground state. Figure 7 shows the potential energy diagram for both the ground and excited states of the $[\text{Ag}(\text{CN})_2^-]_3$ trimer. In Table 2 we summarize the results of the excited-state calculations for the $[\text{Ag}(\text{CN})_2^-]_3$ model at the equilibrium Ag–Ag distance and compare the results with those for the ground state.

Figure 7 shows that a potential well forms in the excited state of $[\text{Ag}(\text{CN})_2^-]_3$ that is about three times deeper than the ground-state potential well. Typical organic exciplexes have binding energies in the vicinity of 10 kcal/mol.⁵¹ The only reported inorganic exciplex formed in solution between $\text{Pt}_2(\text{P}_2\text{O}_5\text{H}_2)_4^{4-}$ and $\text{Tl}(\text{I})$ was determined to have a formation energy slightly less negative than -10 kcal/mol as determined by photoacoustic calorimetry⁵² and optical data.²⁷ The binding energy for the $*[\text{Ag}(\text{CN})_2^-]_3$ exciplex in the title compound is more than four times greater than these values (40.8 kcal/mol) according to our extended Hückel calculations, which implies tremendous thermodynamic stability.

The minimum energy occurs at a Ag–Ag excited-state distance of 2.45 Å. This represents a large excited-state distortion, 0.34 Å shorter than the Ag–Ag equilibrium distance of the ground state and 0.67 Å shorter than the shortest experimental Ag–Ag distance. The formation of excited-state deep potential wells occurring at a shorter internuclear equilibrium distance than the ground state is indicative of exciplex formation.²⁵ However, in the conventional exciplex formation phenomenon in some organic compounds, the ground state has typically been assumed to be structureless with a potential well depth of virtually zero.²⁵ This is not the case for the ground

state in our exciplex model. Figure 7 indicates the presence of weak Ag–Ag interactions in the ground state of the $[\text{Ag}(\text{CN})_2^-]_3$ trimer.

The exciplex model described in this section can effectively explain the luminescence results. The difference in the emission behavior of the two crystallographically distinct Ag sites in the $\text{Tl}[\text{Ag}(\text{CN})_2]$ structure can be explained in terms of excited-state distortion. The $*[\text{Ag}(\text{CN})_2^-]_3$ exciplex is expected to have a shorter Ag–Ag distance than the corresponding ground-state distance in each site (Figure 7). Since the Ag–Ag distance is shorter in the environment of the Ag(1) site than the Ag(2) site, the excited state which is common for both sites is more distorted with respect to the ground state of the Ag(2) site. This agrees with the experimental result that the Ag(2) emission band is broader than the Ag(1) emission (Figure 1). The full-width at half-maximum (fwhm) is about 3.2 and $2.3 \times 10^3 \text{ cm}^{-1}$ for the emission bands with 301 and 318 nm excitation, respectively. These values, according to the above assignment, correspond to the environments of Ag(2) and Ag(1), respectively.

Figure 2 shows that the emission band becomes broader with increasing temperature. The increase of fwhm with increasing temperature can also be attributed to excited-state distortions. The distortion of the excited-state becomes larger at higher temperatures since this is expected to lead to longer Ag–Ag distances (vide supra) and, consequently, broader emission bands.

Exciplex formation in $\text{Tl}[\text{Ag}(\text{CN})_2]$ has resulted in a HOMO–LUMO gap that is 1.25 eV smaller than the gap for isolated $\text{Ag}(\text{CN})_2^-$ ions (Table 2). This result explains the large shift observed in the luminescence spectra of the title compound relative to other Ag(I) species which lack significant Ag–Ag interactions. The HOMO–LUMO gap at the excited-state equilibrium Ag–Ag distance (2.45 Å) is also about 0.3 eV smaller than the gap at the ground-state equilibrium distance of 2.79 Å according to our extended Hückel calculations. This explains the large Stokes shift for the luminescence bands of $\text{Tl}[\text{Ag}(\text{CN})_2]$. The fact is that with such a sizable nuclear rearrangement the emission transition occurs from the exciplex state to the repulsive portion of the ground-state potential curve (Figure 7). Moreover, the results of the aforementioned calculations demonstrate that the excited-state Ag–Ag interactions are more significant than ground-state Ag–Ag interactions.

Conclusions

The experimental and theoretical data in this study indicate that excited-state Ag–Ag interactions are significant in $\text{Tl}[\text{Ag}(\text{CN})_2]$. Ground-state interactions, on the other hand, are less significant in determining the optical properties of the compound. The luminescence of $\text{Tl}[\text{Ag}(\text{CN})_2]$ is attributed to the formation of a silver–silver-bonded exciplex as a result of excited-state Ag–Ag interactions. To our knowledge, this is the first example of a solid-state metal–metal-bound exciplex in coordination compounds.

Acknowledgment. We thank the National Science Foundation for supporting the Molecular Modeling Center at the University of Maine through Grant DUE–9551313. We also wish to thank Professor Raymond C. Fort, Jr., for his help with the ab initio calculations and for his comments on the manuscript.

Supporting Information Available: A table is provided with detailed results of ab initio calculations with a complete bond order analysis according to the Mulliken and Löwdin methods for $[\text{Ag}(\text{CN})_2^-]_3$ trimers with Ag–Ag distances corresponding to the experimental values as well as the minimized geometry (1 page). Ordering information is given on any current masthead page.

(51) Mataga, N.; Torihasa, Y.; Ota, Y. *Chem. Phys. Lett.* **1967**, *1*, 381.

(52) Herman, M. S.; Goodman, J. L. *J. Am. Chem. Soc.* **1989**, *111*, 9105.